International Journal of Robotics and Control Systems
Vol. 5, No. 2, 2025, pp. 698-712
ISSN 2775-2658
http://pubs2.ascee.org/index.php/ijrcs

Design of a Small Wind Turbine Emulator for Testing Power Converters Using dSPACE 1104

T. Boutabba [a,b,1], I. Benlaloui [a,2], F. Mechnane [a,3], I. M. Elzein [c,4], Alfian Ma'arif [d,5], Ammar M. Hassan [e,6], Mohamed Metwally Mahmoud [f,7,*]

[a] LSPIE Laboratory, University of Batna 2, Mostefa Ben Boulaid, Avenue Med Elhadi, Boukhlouf, Algeria
[b] University of Khenchela, El-Hamma, BP 1252 Road of Batna, Khenchela, 40004, Algeria
[c] Department of Electrical Engineering, College of Engineering and Technology, University of Doha for Science and Technology, Doha P.O. Box 24449, Qatar
[d] Department of Electrical Engineering, Universitas Ahmad Dahlan, Yogyakarta, Indonesia
[e] Arab Academy for Science, Technology and Maritime Transport, South Valley Branch, Aswan 81516, Egypt
[f] Electrical Engineering Department, Faculty of Energy Engineering, Aswan University, Aswan 81528, Egypt
[1] boutabba_tarek@yahoo.fr; [2] i.benlaloui@univ-batna2.dz, [3] f.mechnane@univ-batna2.dz, [4] 60101973@udst.edu.qa; [5] alfian.maarif@te.uad.ac.id; [6] ammar@aast.edu; [7] metwally_m@aswu.edu.eg
*Corresponding Author

ARTICLE INFO

Article history
Received October 28, 2024
Revised January 05, 2025
Accepted February 05, 2025

Keywords
Wind Turbine Emulator;
MPPT Control;
dSPACE 1104 Board;
Hardware-In-Loop;
Wind Speed

ABSTRACT

Interest in wind turbine emulators (WTE) has increased due to the growing need for wind power generation as a low-maintenance, more effective substitute for conventional models. This paper presents the design of a small WTE utilizing a dSPACE 1104 system. The setup includes a DC motor, driven by a buck converter, coupled to a permanent magnet synchronous generator, all managed through a hardware-in-the-loop configuration using the dSPACE 1104 board. The DC motor simulates the rotational motion generated by wind energy, accurately replicating the characteristics of an actual WT. This control system enables the simulation of various wind speeds and torque values in MATLAB/Simulink software, providing a valuable tool for analyzing and developing power converters. The results obtained confirmed the effectiveness of the proposed emulator, as the experimental outcomes closely matched the theoretical calculations.

1. Introduction

All over the world in the last decade, research related to renewable energies (extraction, control, distribution, optimization, among others) has increased considerably for two main reasons: on the one hand, the uninterrupted increase in the energy consumption of modern societies; and on the other hand, and as a direct consequence of the previous one, the global need is being generated for eliminating the carbon footprint to mitigate the effects of climate change [1]-[4].

Wind energy (WE) is one of the renewable energies that has gained strength in recent years [5], [6]. To get an idea, at the end of 2015, there was a global installed capacity of about 433 GW [7], [8], due to its high technical maturity, low cost, and non-emission of gas compared to other renewable sources [9]-[11]. The wind turbine (WT) is a mechanical device that converts the flow of wind into rotational energy, which is finally converted into electrical energy by an electric machine [9], [12], [13]. WTs can be found in outlets in the range of watts to MW; in particular, a small WT is considered if it is less than 100 kW. Small WTs are used in low-power applications (residential and clean power), the problem with these WTs is that they generally do not have speed control, which makes it difficult to control the output power [10], [14]. This control has to be done through a power electronic interface that regulates the energy generated by the WT to ensure maximum power extraction [15].

To develop the electronic converters used to control these turbines, it is necessary to use WT emulators (WTEs) to emulate their behavior in laboratory tests [16]-[18]. With WTE, converter designs, and algorithms to monitor the optimal state of the WT under different environmental conditions can be tested, also called maximum power point tracking (MPPT) [19]-[21]. Tests under different environmental conditions are necessary because WE are unpredictable and therefore difficult to manipulate in the laboratory, as there is no standard wind profile for a day of operation; in other words, wind has a random behavior that makes it difficult to know a priori the optimal operating state of the turbine. However, the typical ranges of wind profiles for a geographical location may be known. For example, Colombia has the best wind potential of the Guajira Peninsula because of its wind speeds that vary between 7.4 and 16.6 m/s [22]-[24].

Simulating the average conditions that could occur at a given location involves adopting one of two options for the design of the power treatment system in the WT. The first option is to have a wind tunnel perfectly adapted to the size of the WT you wish to test. This condition is difficult because the instrumentation for this type of solution is complex to guarantee the wind speed required in the specific test. The second option depends on the implementation of an emulation bank with a mechanical coupling between a motor-generator. The generator is a three-phase permanent magnet synchronous generator (PMSG), which is commonly used in small-scale WT applications, the motor is a DC motor and the generator is a three-phase PMSG type [25]-[27]. The WTE takes into account the typical curve of the power coefficient C P (λ, β) of a specific WT, which depends mainly on the wind angle of attack and radius. This WTE makes it possible to test the power output of different WT sizes at different wind speeds without the need for complex instrumentation to ensure correct wind speed.

Therefore, this paper presents the design and implementation of a WE generation system (WEGS) based on the WTE [19]. The WEGS in question is composed of two mechanically coupled electrical machines, one acting as a motor that emulates the rotational motion due to wind dynamics in the WT and the other acting as a generator [28]. This work presents a WTE, having a main machine DC motor driven by a buck converter, and a control system in hardware-in-the-loop (HIL) configuration based on dSPACE 1104 card. For the modeling of the wind power system, MATLAB® / Simulink® software has been used, taking into account all the characteristics of a real WT. For the communication between the microcomputer and the experimental bench, a DSP320F28335 microcontroller from the manufacturer Texas Instruments was used. The results obtained demonstrated the efficiency of the proposed WTE, given that the behavior of the experimental bench was the same as that of the theoretical calculation results.

This work has been prepared to be in four sections after the introduction section. Section 2 presents the wind dynamics in WTs and the applied MPPT technique. Section 3 presents the needed materials and methods. Section 4 presents the obtained results to prove the accuracy of the studied WTE. Section 5 concludes the current study.

2. Wind Dynamics in WTs and MPPT Technique

The understanding of wind dynamics in WTs has great importance, because WTs have a higher efficiency due to the restrictions imposed by Betz's limit [22], [29]; i.e. no three-bladed cross-section WT has an efficiency higher than the maximum possible efficiency according to the power coefficient (C_p) curve (0.593), i.e. how much of the effective wind power can be transferred to the mechanical power in the WT rotor; this restriction is physically explained in [22], [30], [31]. After several tests with rotors connected to the WTs and a sweep of the wind speeds, graphs of the $C_p$versus blade tip speed are obtained at different angles of β, examples of the three-bladed WTs are shown in Fig. 1.

Also, the general model of the WT rotor (equation (1)) was taken from [17], [32], [33], in which the C_p equation (equation (2)) is presented; it is a relationship between WE and the mechanical power that is transferred to the turbine rotor. Equation (2) applies to all three-bladed turbines in which the parameters C_i (i=1.. 6) have been found utilizing a regression algorithm. In addition, in equation (2) β is the angle of attack of the blade cross-section concerning the wind direction; in small-scale WTs, this value is fixed and is generally close to zero because, according to Fig. 1, this is the angle at which the WT achieves the highest efficiency. λ_i is a relationship represented in equation (3) and λ is the WT blade tip speed which depends proportionally on the blade radius in m. ω is the angular velocity of the turbine rotor with units in rad / s, and inversely proportional to the wind speed V_{wind} in m/s as seen in equation (3):

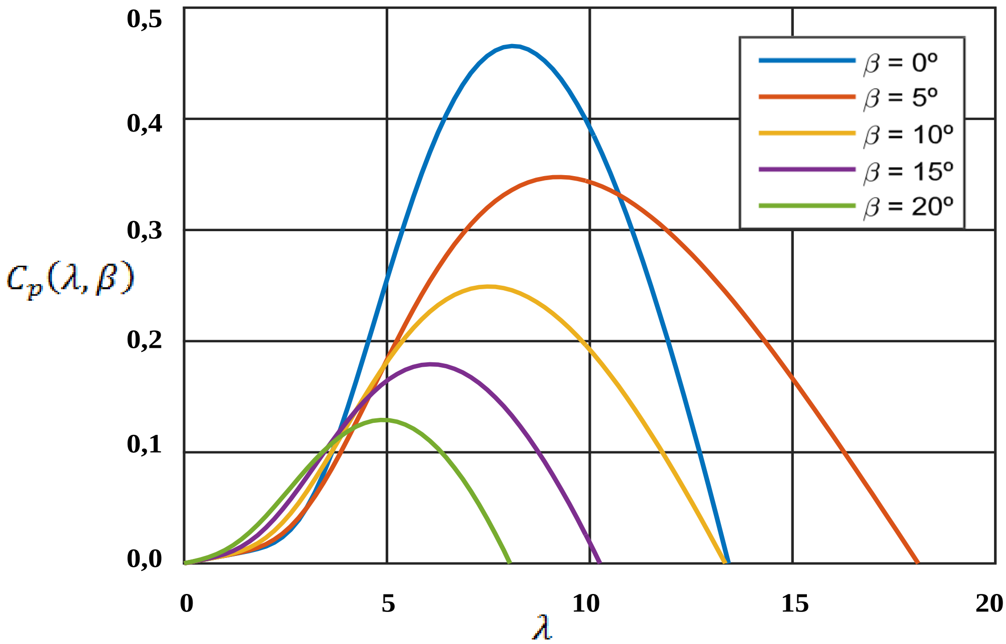

Fig. 1. Power coefficient for different values of λ

$$P_m = C_p(\lambda,\beta)\left(\frac{1}{2}\rho A v_v^3\right) = C_p(\lambda,\beta)\left(\frac{1}{2}\rho\pi R^2 v_v^3\right) \tag{1}$$

$$C_p(\lambda,\beta) = C_1\left(\frac{C_2}{\lambda_i} - C_3\beta - C_4\right)e^{-C_5/\lambda_i} + C_6\lambda_i \tag{2}$$

Where it is defined as

$$\frac{1}{\lambda_i} = \left[\left(\frac{1}{\lambda + c_6\beta}\right) - \left(\frac{c_9}{\beta^3 + 1}\right)\right] \tag{3}$$

The c_1-c_9 coefficients are designed and adapted to describe a specific turbine. To calculate the λ at the end of the blade, the expression given in [12] as presented in equation (4) is used, where ω_r is the angular velocity of the rotor in (rad/s). Fig. 2 shows typical values of *Cp (λ)* for different wind rotors as a function of λ.

$$\lambda = \frac{R\omega_r}{V} \tag{4}$$

It should be clarified that in our case, the developed WTE considers the WT controlled by stall or with control by aerodynamic design (stall control), where the pitch angle remains constant during the entire turbine operation, and therefore, the C_p will depend only on the specific speed coefficient λ, therefore the values in Fig. 2 are considered valid.

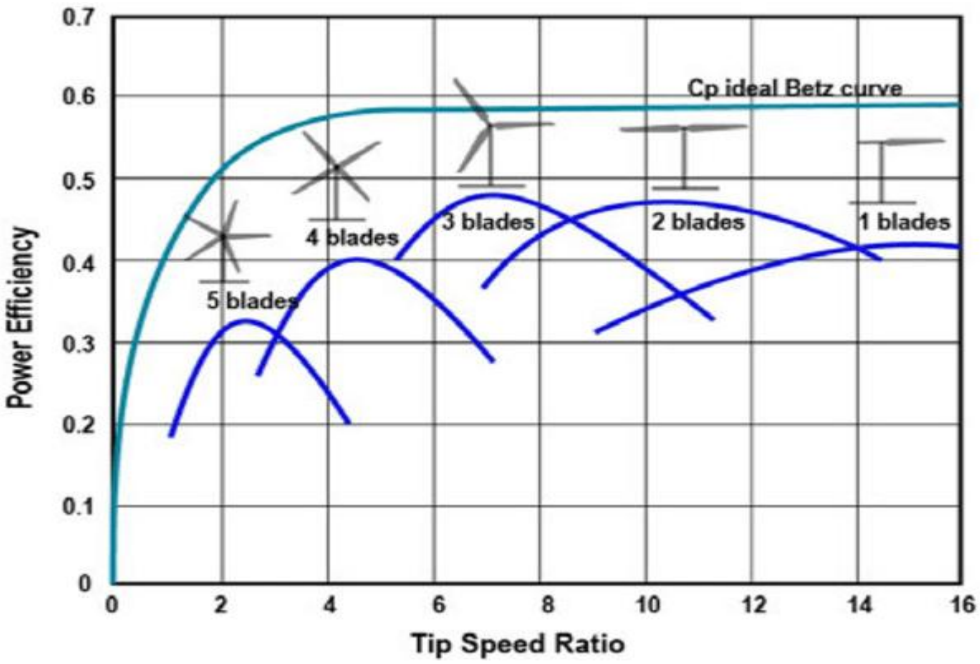

Fig. 2. C_p for different models of WTs as a function of λ

To determine an analytical expression of the C_p of the WTs to be emulated, which are one-bladed, two-bladed, three-bladed, and Darrius, we looked for 3rd order polynomials as in Table 1, that represent the curves in Fig. 2 as a function of the λ which will be one of the input variables of the emulator control program, obtaining the following system of equations.

Table 1. The analytical expression of the C_p of the WTs

Type	C_p equation	λ equation
One-Blade	Cp (λ)=−0,00002λ−0,0023λ + 0,0819λ − 0,2309	For 9,1≤λ ≤ 18
Two-Blade	Cp (λ)= 0,0005λ− 0,0227λ + 0,2984λ − 0,7782	For 6,9≤λ≤ 14,5
Three-Blade	Cp (λ)= 0,0023λ − 0,069λ + 0,6321λ − 1,3542	For 5,3≤λ≤ 11,2
Darrius	Cp (λ)= 0,0052λ − 0,1181λ + 0,7984λ − 1,2952	For 3,4≤λ≤ 7,4

Applying equation (1) and considering the speed of rotation of the WT (ω), it is possible to determine the mechanical torque exerted by it (T) employing the following equation:

$$\tau_r = \frac{P_{wind}\, C_p(\lambda)}{\omega_r} \tag{5}$$

Finally, substituting the parameter Cp (λ) in equation (5) with equations in Table 1 as appropriate, it is possible to obtain the torque generated by a WT as a function of the parameters air density (ρ), wind speed (v), radius of gyration (R), height (H) (for the Derrius rotor) and specific speed (λ) of the four models considered as shown in equations (6) and (7), then they will be used as equations of "torque to develop" in the impulse motor that simulates these turbines.

$$\tau_{rotor} = \frac{C_p(\lambda) P_{wind}}{\omega_r} = \frac{\rho \pi R^3 v_v^3 C_p(\lambda)}{2\lambda} \tag{6}$$

$$\tau_{rotor} = \frac{0.67 \rho R^2 v_v^2 H C_p(\lambda)}{\lambda} \rightarrow \text{Darrieus} \tag{7}$$

One of the most widely used techniques in the literature for maximizing power extraction in renewable energy sources is tip speed ratio control (TSR) [34]-[36]. In this method, the maximum power of the wind turbine is obtained by maintaining the speed ratio at the end of the blade λ at its ideal value λ_0. The principle of operation of the MPPT technique with an optimal speed ratio at the tip of the blade is illustrated in Fig. 3 [36], [37], in which the wind speed V_{wind} is measured and used to calculate the reference speed ω_r Generator as a function of the optimal ratio λ_0 and the turbine speed ratio n_{BV} / n_{AV}. The speed of the generator is controlled by power converters and will be equal to its steady state reference, in which the MPPT is reached.

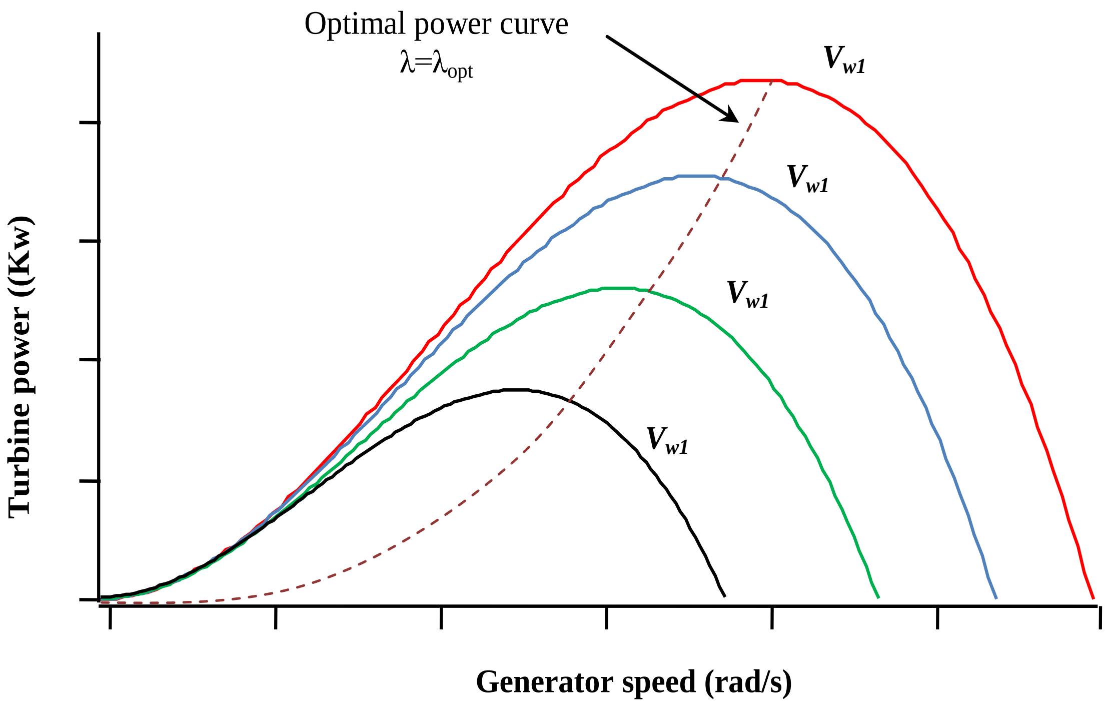

Fig. 3. Characteristics of turbine power as a function of the rotor speed for a series of wind speeds

3. Materials and Methods

3.1. WTE Method

The emulation of a WT must be configured, as shown in Fig. 4. This scheme presents a motor-generator coupling for the emulation of a WT that considers the characteristics of the system. This system requires the calculation of the reference angular speed of the engine given by equation (8).

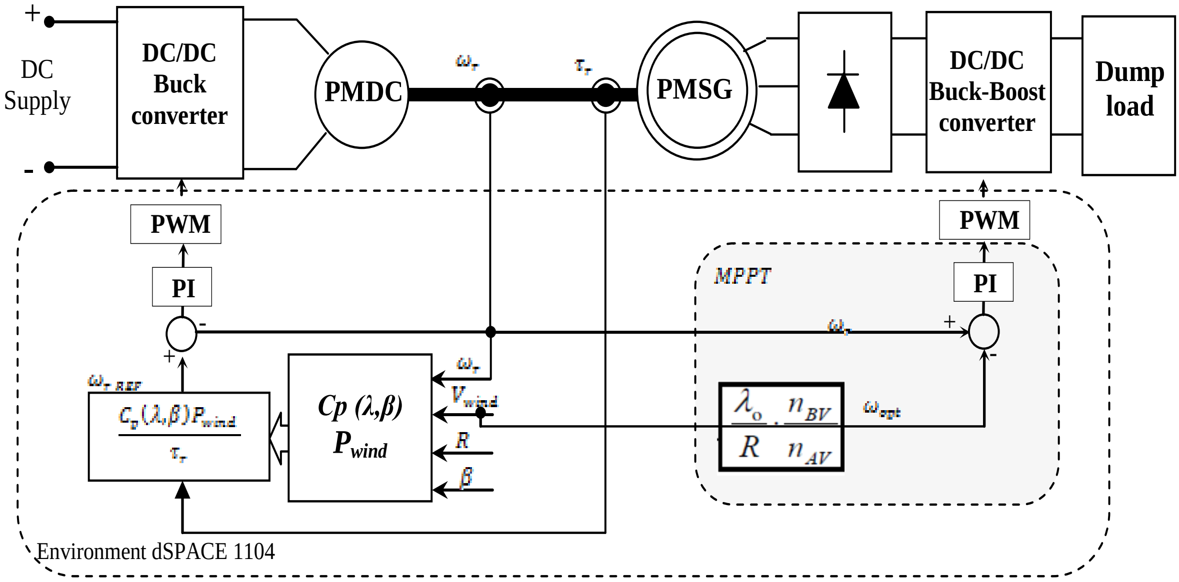

Fig. 4. The WTE interface

$$\omega_r = \frac{P_{wind\ C_p(\lambda,\beta)}}{\tau_r} \quad (8)$$

The system requires the acquisition of the torque measurement τ_r (nm newton meter), the calculation of the power generated by the P_{wind} (W), and the power coefficient C_p (λ, β) (non-dimensional), as indicated in [38]-[40]. Also, the calculation of the reference speed ω_{ref} (rad /s) should be applied to the DC motor speed control board to ensure correct emulation of the required wind conditions.

It should be noted that the processing of measured information of the motor-generator coupling should be processed in real-time by an acquisition system that allows you to make the necessary variations to emulate real conditions. This interface can be implemented with typical signal processing devices (acquisition cards, dSPACE, etc.). As presented in later sections, the system implemented for the emulation platform consists of a dSPACE 1104 control system as an acquisition card, which in turn sends the data to the control desk for processing and interaction.

Fig. 5 shows the procedure to emulate the complete wind system. Its main input is the specific wind speed to be emulated and is given by the user, also is given by the system constants as the parameters of Cp (λ, β), the rotor radius, and the air density ρ_{air}. Some variables are also entered but not given by the user but acquired by sensors, such as torque measurement and angular speed and finally the output is the reference speed that is applied to the card that controls the speed of the DC motor ω_{ref}.

3.2. Mathematical Modeling of the Switched Converter

Since the wind turbine generates voltages lower than those demanded by the load, the suitable converter for the application is a DC-DC converter buck-up, which is coupled after a three-phase rectifier bridge with its respective filtering capacitor C_{in} [41]-[43]. The main function of this converter is to condition the power of the WT and in this case, deliver it to a resistive load, depending on the required voltage levels in the output capacitor C_o; typically, the control that is designed for this type of application is the PI controller [44]-[46].

The step-up DC-DC converter of Fig. 6, whose mathematical model is given by the averaged model, has three active elements that are: inductance, input capacitor, and output capacitor, which are associated with the three states of the converter, the coil current $i_L(t)$; the input capacitor voltage v_{Cin} (t); and the output capacitor voltage v_{C0} (t), vC0 (t), vCin (t), iL(t) [47].

From the modeling of converters for control purposes presented in [48], a mathematical representation in state space can be obtained, as shown in equation (9).

$$\dot{x(t)} = \begin{bmatrix} 0 & -\frac{1}{C_{in}} & 0 \\ \frac{1}{L} & 0 & -\frac{(1-d)}{L} \\ 0 & \frac{(1-d)}{C_0} & -\frac{1}{R_0 C_0} \end{bmatrix} x(t) + \begin{pmatrix} -\frac{i_{in}}{C_{in}} \\ 0 \\ 0 \end{pmatrix} \quad (9)$$

For this case, the state space is presented as a function of regulating the power extraction of the wind turbine, that is, it is desired to control the input current to the converter associated with the coil current $i_L(t)$; Likewise, the states of the system x (t) are made up of v_{Cin} (t), $iL(t)$t and vC_0 (t). Taking into account the nonlinearity of the system, a linear approximation to the model evaluated at equilibrium is required to guarantee the correct design of a PI controller, as proposed in [49]. The equilibrium points of the system can be predicted when the converter has stabilized, that is when $\dot{x(t)} = 0$, thus $V^*_{C_{in}}(t) = (1-D)^2 R_0 i_{in}$, $I^*_L = i_{in}$, $V^*_{C_0}(t) = (1-D) R_0 i_{in}$.

These values are replaced in the linear model evaluated at the equilibrium points. From the model presented in equation (10), we proceed to design a PI controller that meets the desired criteria for regulating the converter current from a reference given by an MPPT algorithm.

$$\dot{x}(t) = \begin{bmatrix} 0 & -\frac{1}{C_{in}} & 0 \\ \frac{1}{L} & 0 & -\frac{(1-d)}{L} \\ 0 & \frac{(1-d)}{C_0} & -\frac{1}{R_0 C_0} \end{bmatrix} x(t) + \begin{pmatrix} 0 \\ \frac{V_{C_0}^*}{L} \\ -\frac{I_L^*}{C_0} \end{pmatrix} d(t) \tag{10}$$

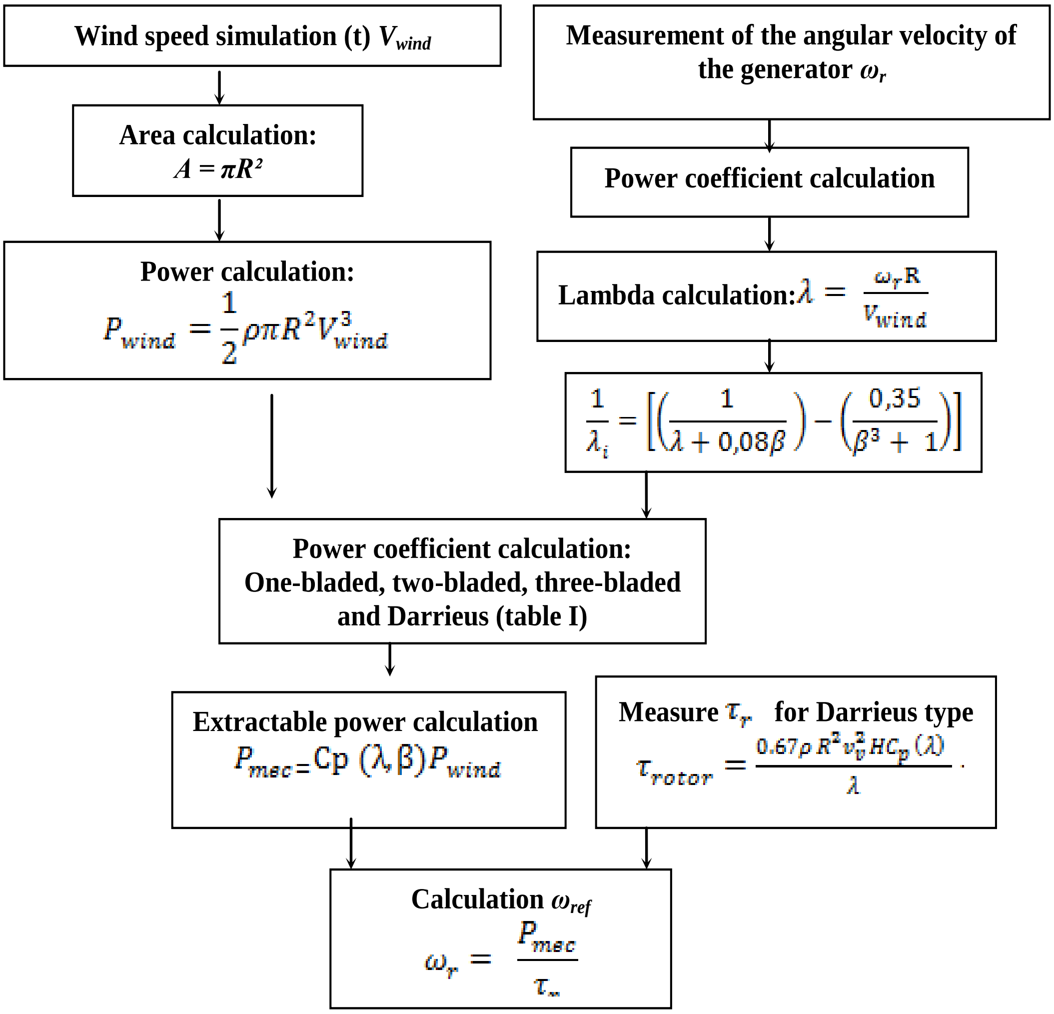

Fig. 5. Procedure for emulating the WT

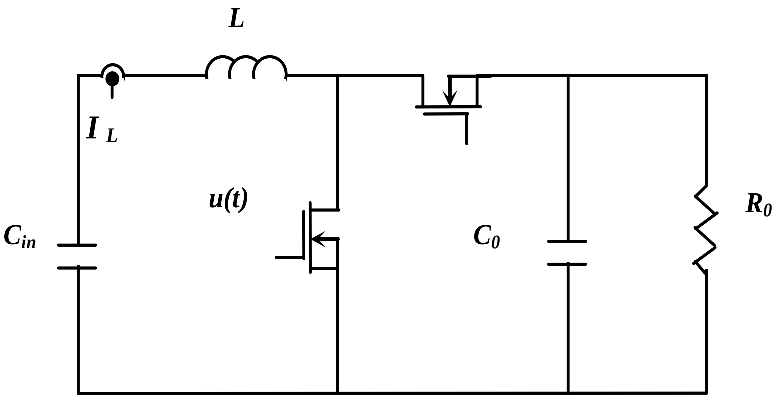

Fig. 6. Boost DC-DC converter diagram

4. Results and Discussions

4.1. Implementation of a WTE Platform with an MPPT Algorithm

Fig. 7 presents a motor-generator bank, the DC motor is controlled employing a speed controller from the dSPACE 1104, this measures the feedback using a current and voltage sensor used to estimate speed value and delivers a DC voltage proportional to rotor speed. The generator is coupled to the motor with a ball screw shaft flexible coupling, in addition, the angular velocity and torque values were acquired with a control desk card, in which the reading is done through each of the ADC ports; likewise, the analog signals with filtered PWM ports, necessary to monitor the reference angular velocity ω_{ref} and the power coefficient C_P (λ, β), are reproduced. The PMSG and DC motor parameters are listed in Table 2.

Table 2. PMSG and DC motor parameters

PMSG		PMDC
P=220 W L_d =0.00012 H J=0.0016 Kg m^2 V_n=24 V I_n=13.6 A	R=0.0675 Ω, L_q =0.0008 H φ_f=0.0441 Wb P=3 C_n=5 N.m, f = 388.18*10^{-6} Nm/s	V_n=24 V I_n=9~11 A P=250 W N=2650 RPM C_n=5 N.m

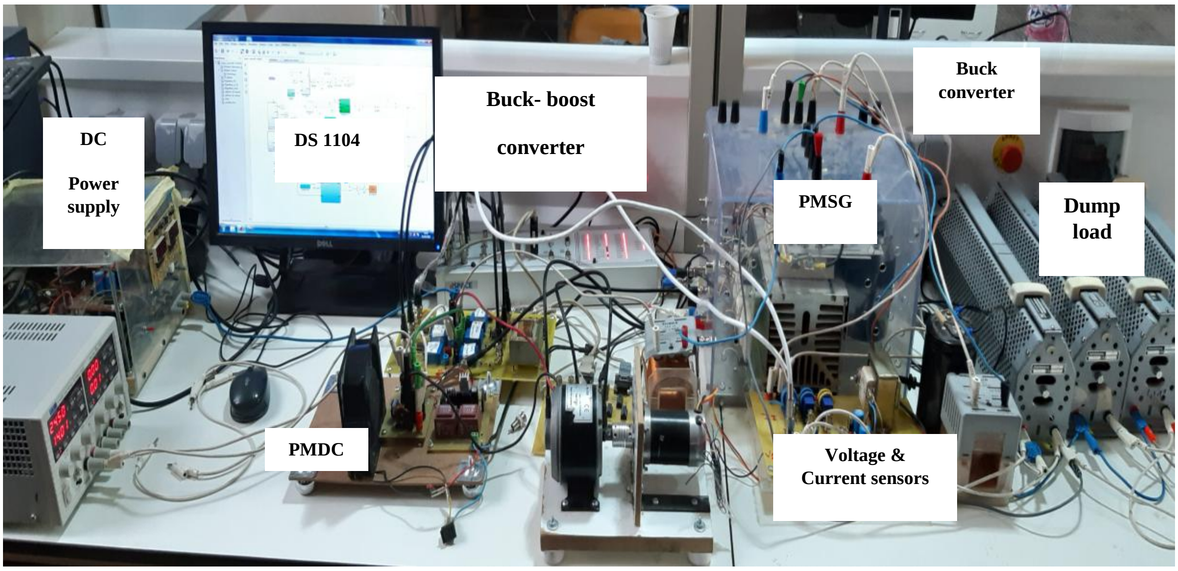

Fig. 7. The hardware setup of the system

Fig. 8 presents the complete emulation platform considering the power electronics interface and the MPPT algorithm. Also, a 3-phase rectifier is connected to the generator terminals which have a filtering capacitor of the rectified signal, and then a boost type converter which is controlled with a PI controller to regulate current. This controller is designed to follow the speed references delivered by the MPPT algorithm in search of a maximum power point; both the control and the MPPT algorithm are implemented in the dSPACE 1104 card.

4.2. Experimental Results

The experimental platform was configured to emulate types of WTs (one-blade, two-blade, three-blade, and Darrius) in particular conditions in which the coefficients for the calculation of the power coefficient are given in Table 1. These parameters allow the emulation of these turbines. These results illustrate the WT's response to a random wind profile presented in Fig. 9, in which the WT rotation follows this wind variation. Thus, observing that the estimated mechanical power of the WTs and the power generated depend on the WT rotation (since the rotation determines the WT operating point in the C_p versus TSR curve) and, consequently, also following the wind variation. The C_p is practically constant, which is characteristic of operation at the MPP. The oscillations presented in Cp are due to abrupt variations in wind speed, causing its TSR to assume high values for fractions of a second, as a result of the turbine rotating at high speed and soon the wind suffers a sharp drop, as predicted by Equation (4).

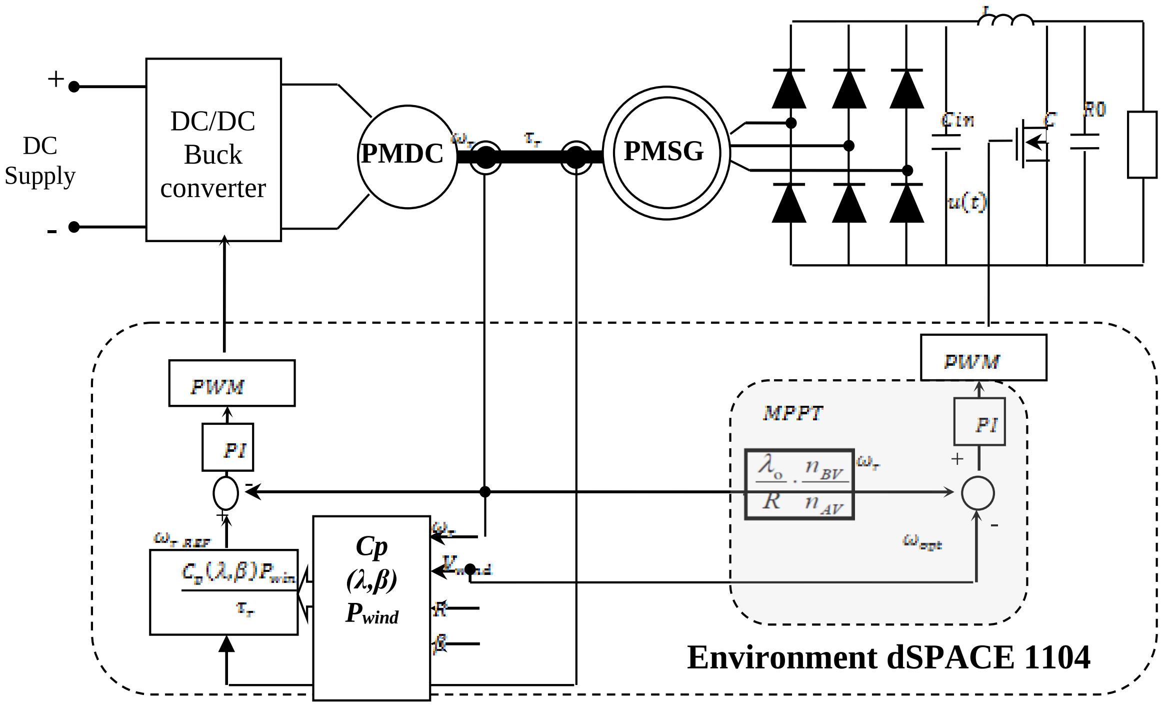

Fig. 8. The complete emulation platform with the power electronics interface and the MPPT algorithm

From the procedure presented in [50], [49], [51], a PI controller was designed for the speed loop of a boost converter. The idea of implementing a search algorithm for the MPP, type TSR control, requires that the variable delivered by it serves as a reference for a controller of a switched converter (in this case it is a speed control), the control is a controller PI in discrete time since it is implemented in a digital signal processor, together with the MPPT algorithm.

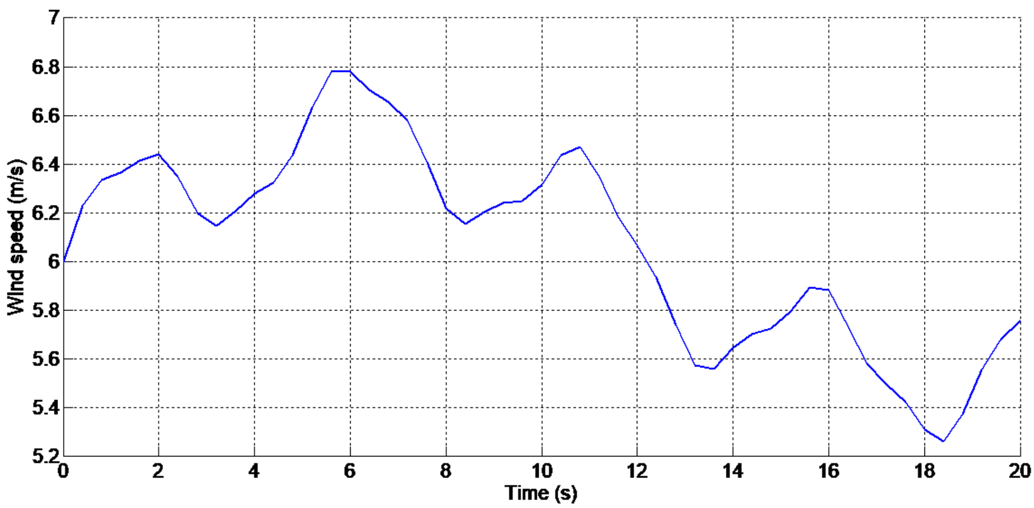

Fig. 9. Wind speed signal

Fig. 10 shows the results of the *Cp* simulations for the different types of wind turbines presented in the previous section. For the system in question, the ideal would be that the value of *Cp* is always stable, reaching very close values even with many variations of the wind value. The three-bladed WT and the Darrius both have an average Cp value very close to 0.3 throughout the simulation and, therefore, for the entire range of wind speeds visualized in Fig. 9. The C_p of the WT with wind value variation is shown in Fig. 11. Where the $C_p(\lambda,\beta)$ Parameters C_i (i=1.. 6) in equation (3) are chosen to fit very small power WT.

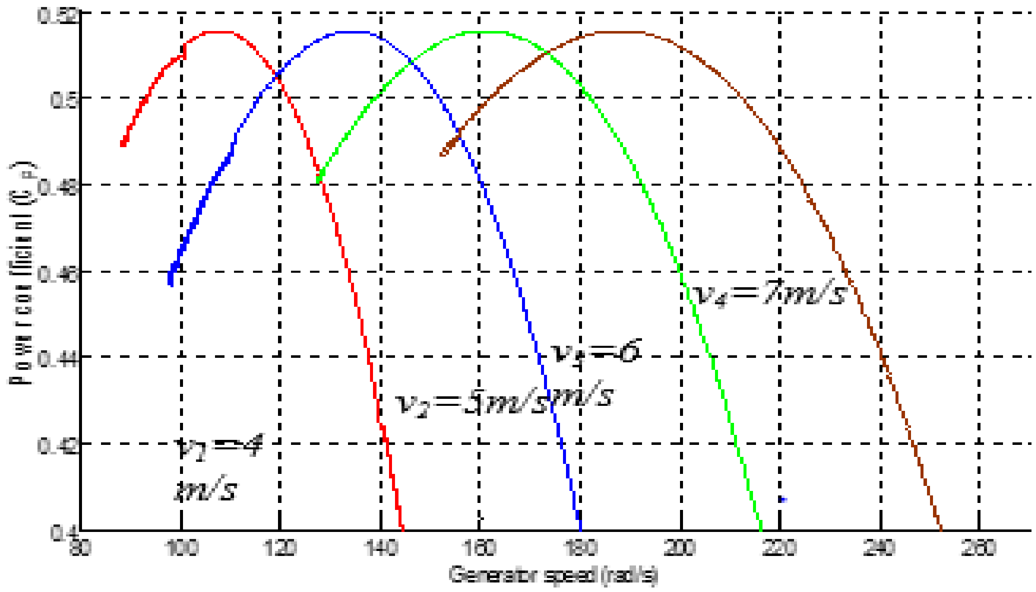

Fig. 10. Characteristics of turbine power as a function of the rotor speed for a series of wind speeds

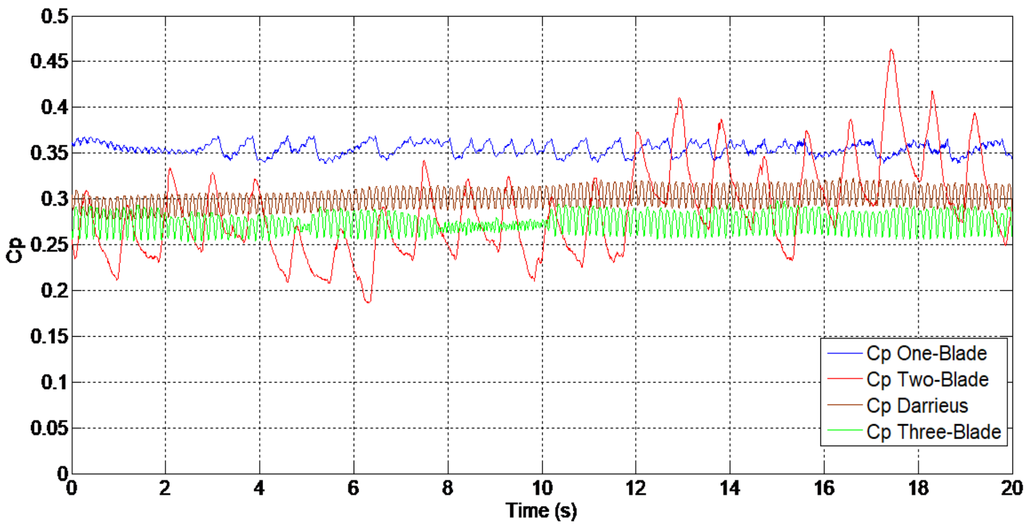

Fig. 11. Response of the power coefficient

In Fig. 12 and Fig. 13, the results of the simulations of the estimated torque values and the wind power for the different WTs presented in the previous section are presented. The values of these torques and powers are relatively close for the four emulated WTs. It can be seen that for the three-bladed and Derrius WTs, the value of the estimated torques and wind power are very close and higher than the one-bladed and two-bladed wind turbines, due to the high value of Cp of these two see Table 1. Fig. 14 shows the response of the generated DC voltage of the four emulated WTs, which is proportional to rotor speed and with a random wind profile.

The corresponding windmill speed ω_g, estimated rotational speed ω_{est}, and the optimal speed are shown in Fig. 15. It is observed that with a variable wind speed Fig. 9, the motor speed follows the estimated rotor speed. To investigate the maximum power extraction from the developed small WTE, the TSR was recorded for this variation in wind speed. The TSR reached the optimum TSR (ω_{opt}) along with the variation of the wind.

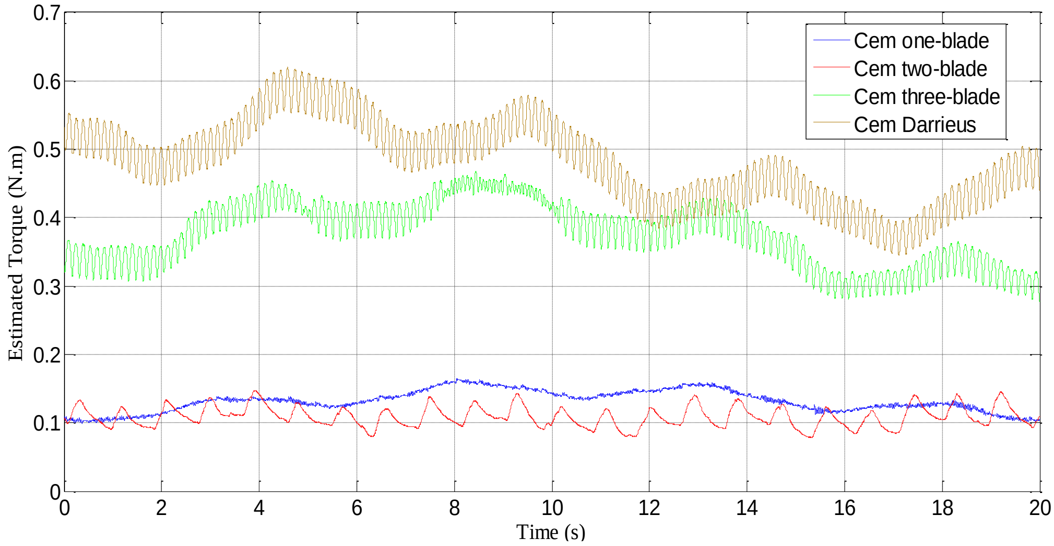

Fig. 12. Response of the estimated torque

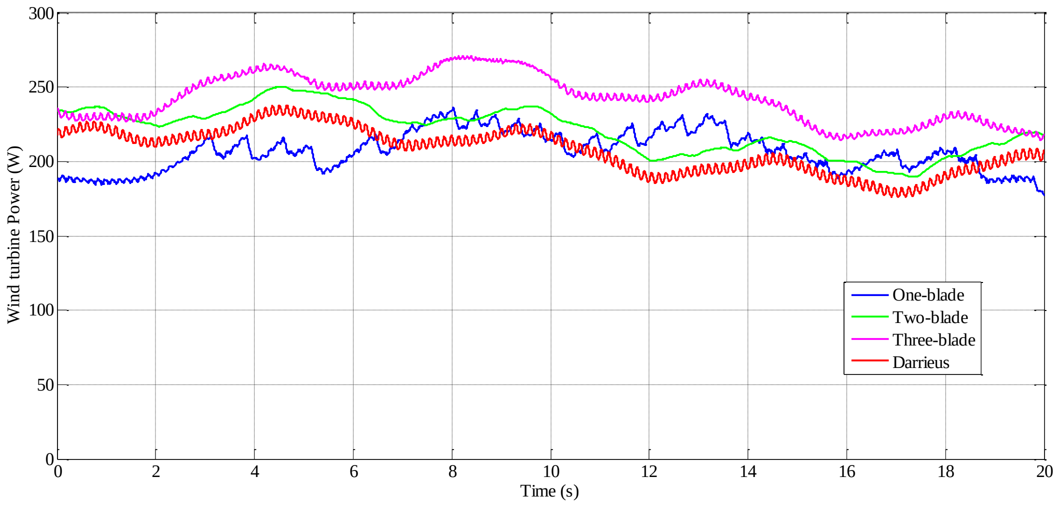

Fig. 13. WT power

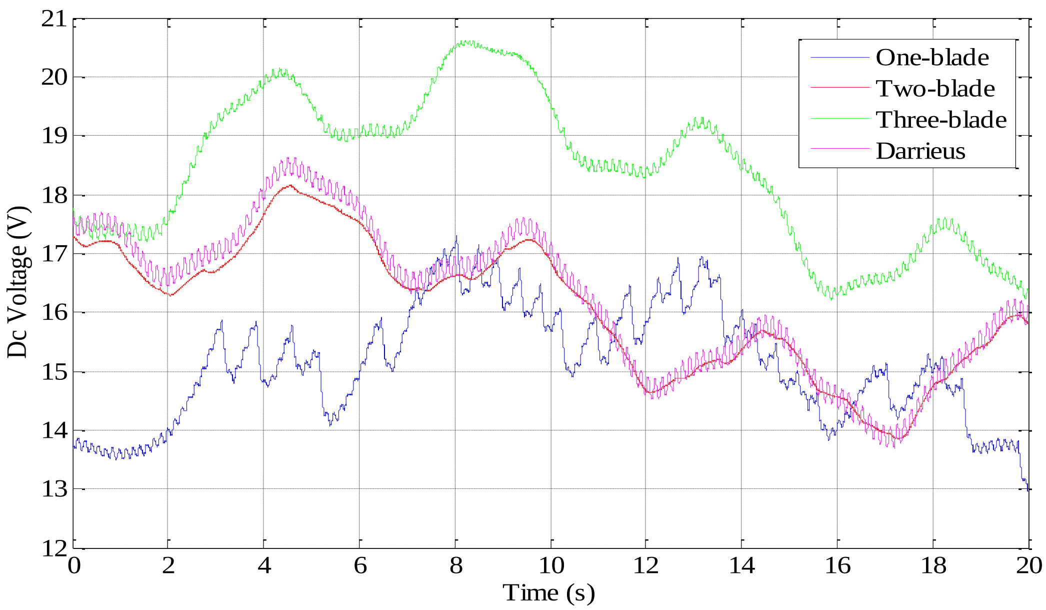

Fig. 14. Response of generated DC voltage

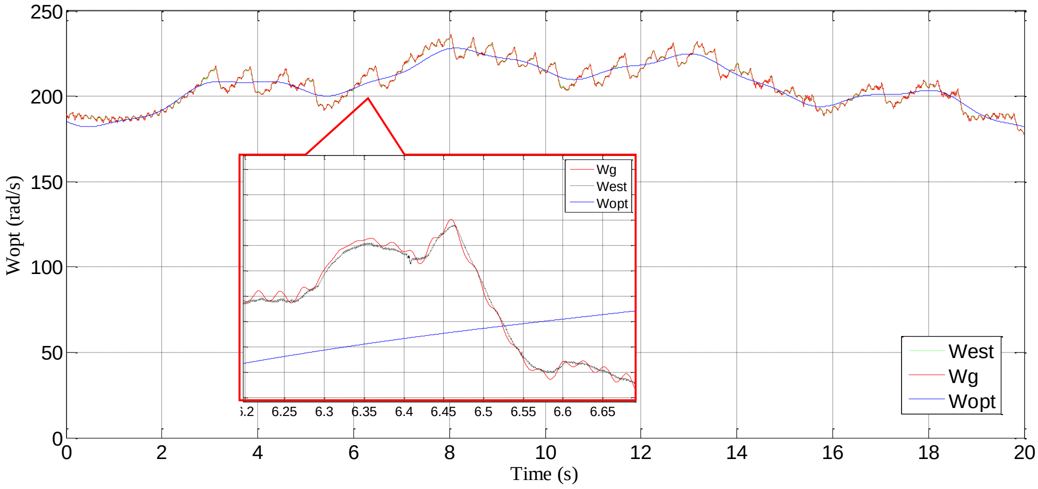

Fig. 15. Response of the rotor speed under variable wind speed

5. Conclusions

In this work, an emulator bench was presented that reproduces the behavior of a WT under different wind profiles and load conditions, thus becoming independent of the existence of weather conditions that allow the test to be carried out. The type of WT can be configured simply by incorporating the corresponding polynomial coefficients in the control system that controls the variable speed drive. From the review of the cited references, the theoretical calculations carried out and the simulations and experimental tests carried out, the following conclusions can be drawn:

a) A new system has been presented for the emulation of different kinds of WTs, consisting of the series interconnection of a variable DC voltage source, a resistor of power, and a permanent magnetic DC motor and PMSG;

b) It has been shown, through theoretical developments, simulations, and experimental tests, that the emulator can reproduce the power curves of a WT;

c) The presented emulator is useful for carrying out laboratory tests of the power converters used to control the WT generator;

d) The novelty of the emulator consists of working in an open loop, while speed emulators work in a closed loop, so the proposed emulator has an intrinsic structure more like WTs.

Author Contribution: All authors contributed equally to the main contributor to this paper. All authors read and approved the final paper.

Data Availability: The data used to support the findings of this study are available at reasonable request from the corresponding author.

Conflicts of Interest: The authors declare that they have no conflicts of interest.

Funding: This research received no external funding

References

[1] Z. Wang, S. Li, Z. Jin, Z. Li, Q. Liu, and K. Zhang, "Oil and gas pathway to net-zero: Review and outlook," *Energy Strategy Reviews*, vol. 45, p. 101048, 2023, https://doi.org/10.1016/j.esr.2022.101048.

[2] M. Awad *et al.*, "A review of water electrolysis for green hydrogen generation considering PV/wind/hybrid/hydropower/geothermal/tidal and wave/biogas energy systems, economic analysis, and its application," *Alexandria Engineering Journal*, vol. 87, pp. 213–239, 2024, https://doi.org/10.1016/j.aej.2023.12.032.

[3] G. Chen, A. Bahrami and M. Narimani, "A New Seven-Level Topology for High-Power Medium-Voltage Application," *IEEE Transactions on Industrial Electronics*, vol. 68, no. 1, pp. 37-46, 2021, https://doi.org/10.1109/TIE.2019.2962456.

[4] A. M *et al*., "Prediction of Optimum Operating Parameters to Enhance the Performance of PEMFC Using Machine Learning Algorithms," *Energy Exploration & Exploitation*, 2024, https://doi.org/10.1177/01445987241290535.

[5] M. M. Mahmoud, "Improved current control loops in wind side converter with the support of wild horse optimizer for enhancing the dynamic performance of PMSG-based wind generation system," *International Journal of Modelling and Simulation*, vol. 43, no. 6, pp. 952-966, 2023, https://doi.org/10.1080/02286203.2022.2139128.

[6] M. M. Mahmoud, M. Khalid Ratib, M. M. Aly, and A. M. M. Abdel-Rahim, "Wind-driven permanent magnet synchronous generators connected to a power grid: Existing perspective and future aspects," *Wind Engineering*, vol. 46, no. 1, pp. 189–199, 2022, https://doi.org/10.1177/0309524X211022728.

[7] L. Dong, W. H. Lio, and G. R. Pirrung, "Analysis and design of an adaptive turbulence-based controller for wind turbines," *Renewable Energy*, vol. 178, pp. 730–744, 2021, https://doi.org/10.1016/j.renene.2021.06.080.

[8] M. M. Mahmoud *et al*., "Application of Whale Optimization Algorithm Based FOPI Controllers for STATCOM and UPQC to Mitigate Harmonics and Voltage Instability in Modern Distribution Power Grids," *Axioms*, vol. 12, no. 5, p. 420, 2023, https://doi.org/10.3390/axioms12050420.

[9] O. Dahhani, A. El-Jouni, and I. Boumhidi, "Assessment and control of wind turbine by support vector machines," *Sustainable Energy Technologies and Assessments*, vol. 27, pp. 167–179, 2018, https://doi.org/10.1016/j.seta.2018.04.006.

[10] A. Bonfiglio, F. Delfino, F. Gonzalez-Longatt, and R. Procopio, "Steady-state assessments of PMSGs in wind generating units," *International Journal of Electrical Power & Energy Systems*, vol. 90, pp. 87–93, 2017, https://doi.org/10.1016/j.ijepes.2017.02.002.

[11] M. M. Mahmoud *et al*., "Evaluation and Comparison of Different Methods for Improving Fault Ride-Through Capability in Grid-Tied Permanent Magnet Synchronous Wind Generators," *International Transactions on Electrical Energy Systems*, vol. 2023, no. 1, pp. 1-22, 2023, https://doi.org/10.1155/2023/7717070.

[12] Z. Maheshwari, K. Kengne, and O. Bhat, "A comprehensive review on wind turbine emulators," *Renewable and Sustainable Energy Reviews*, vol. 180, p. 113297, 2023, https://doi.org/10.1016/j.rser.2023.113297.

[13] M. N. A. Hamid *et al*., "Adaptive Frequency Control of an Isolated Microgrids Implementing Different Recent Optimization Techniques," *International Journal of Robotics and Control Systems*, vol. 4, no. 3, pp. 1000–1012, 2024, https://doi.org/10.31763/ijrcs.v4i3.1432.

[14] M. A. Bhayo *et al*., "An Experimental Hybrid Control Approach for Wind Turbine Emulator," *IEEE Access*, vol. 11, pp. 58064-58077, 2023, https://doi.org/10.1109/ACCESS.2023.3283420.

[15] A. Shafiei, B. M. Dehkordi, A. Kiyoumarsi and S. Farhangi, "A Control Approach for a Small-Scale PMSG-Based WECS in the Whole Wind Speed Range," *IEEE Transactions on Power Electronics*, vol. 32, no. 12, pp. 9117-9130, 2017, https://doi.org/10.1109/TPEL.2017.2655940.

[16] I. Moussa and A. Khedher, "A Theoretical and Experimental Study of a Laboratory Wind Turbine Emulator using DC-Motor Controlled by an FPGA-Based Approach," *Electric Power Components and Systems*, vol. 48, no. 4–5, pp. 399–409, 2020, https://doi.org/10.1080/15325008.2020.1793834.

[17] F. Martinez, L. C. Herrero, and S. de Pablo, "Open loop wind turbine emulator," *Renewable Energy*, vol. 63, pp. 212–221, 2014, https://doi.org/10.1016/j.renene.2013.09.019.

[18] S. Rajendran, M. Diaz, V. S. K. Devi, D. Jena, J. C. Travieso, and J. Rodriguez, "Wind Turbine Emulators—A Review," *Processes*, vol. 11, no. 3, p. 747, 2023, https://doi.org/10.3390/pr11030747.

[19] J. C. Y. Hui, A. Bakhshai and P. K. Jain, "An Energy Management Scheme With Power Limit Capability and an Adaptive Maximum Power Point Tracking for Small Standalone PMSG Wind Energy Systems," *IEEE Transactions on Power Electronics*, vol. 31, no. 7, pp. 4861-4875, 2016, https://doi.org/10.1109/TPEL.2015.2478402.

[20] B. S. Atia *et al.*, “Applications of Kepler Algorithm-Based Controller for DC Chopper: Towards Stabilizing Wind Driven PMSGs under Nonstandard Voltages,” *Sustainability*, vol. 16, no. 7, p. 2952, 2024, https://doi.org/10.3390/su16072952.

[21] F. Menzri, T. Boutabba, I. Benlaloui, H. Bawayan, M. I. Mosaad, and M. M. Mahmoud, “Applications of hybrid SMC and FLC for augmentation of MPPT method in a wind-PV-battery configuration,” *Wind Engineering*, vol. 48, no. 6, pp. 1186-1202, 2024, https://doi.org/10.1177/0309524X241254364.

[22] J. M. Mejía, F. Chejne, R. Smith, L. F. Rodríguez, O. Fernández, and I. Dyner, “Simulation of wind energy output at Guajira, Colombia,” *Renewable Energy*, vol. 31, no. 3, pp. 383–399, 2006, https://doi.org/10.1016/j.renene.2005.03.014.

[23] H. Boudjemai *et al.*, “Application of a Novel Synergetic Control for Optimal Power Extraction of a Small-Scale Wind Generation System with Variable Loads and Wind Speeds,” *Symmetry*, vol. 15, no. 2, p. 369, 2023, https://doi.org/10.3390/sym15020369.

[24] N. F. Ibrahim *et al.*, “Multiport Converter Utility Interface with a High-Frequency Link for Interfacing Clean Energy Sources (PV\Wind\Fuel Cell) and Battery to the Power System: Application of the HHA Algorithm,” *Sustainability*, vol. 15, no. 18, p. 13716, 2023, https://doi.org/10.3390/su151813716.

[25] H. Boudjemai *et al.*, "Experimental Analysis of a New Low Power Wind Turbine Emulator Using a DC Machine and Advanced Method for Maximum Wind Power Capture," *IEEE Access*, vol. 11, pp. 92225-92241, 2023, https://doi.org/10.1109/ACCESS.2023.3308040.

[26] N. A. N. Aldin, W. S. E. Abdellatif, Z. M. S. Elbarbary, A. I. Omar and M. M. Mahmoud, "Robust Speed Controller for PMSG Wind System Based on Harris Hawks Optimization via Wind Speed Estimation: A Real Case Study," *IEEE Access*, vol. 11, pp. 5929-5943, 2023, https://doi.org/10.1109/ACCESS.2023.3234996.

[27] H. Alnami, S. A. E. M. Ardjoun, and M. M. Mahmoud, “Design, implementation, and experimental validation of a new low-cost sensorless wind turbine emulator: Applications for small-scale turbines,” *Wind Engineering*, vol. 48, no. 4, pp. 565-579, 2024, https://doi.org/10.1177/0309524X231225776.

[28] J. Castelló, J. M. Espí, and R. García-Gil, “Development details and performance assessment of a Wind Turbine Emulator,” *Renewable Energy*, vol. 86, pp. 848–857, 2016, https://doi.org/10.1016/j.renene.2015.09.010.

[29] Y. Aljarhizi, A. Nouaiti, E. Al Ibrahmi, C. Boutahiri, A. Hassoune, and A. Mesbahi, “Optimized Wind Turbine Emulator based on an AC to DC Motor Generator Set,” *Engineering, Technology & Applied Science Research*, vol. 13, no. 2, pp. 10559–10564, 2023, https://doi.org/10.48084/etasr.5775.

[30] J. R. de Oliveira and A. L. Andreoli, "Wind Turbine Emulator: A Tool for Experimental and Computational Study," *IEEE Latin America Transactions*, vol. 19, no. 11, pp. 1832-1839, 2021, https://doi.org/10.1109/TLA.2021.9475616.

[31] M. M. Mahmoud, M. M. Aly, H. S. Salama, and A. M. M. Abdel-Rahim, “An internal parallel capacitor control strategy for DC-link voltage stabilization of PMSG-based wind turbine under various fault conditions,” *Wind Engineering*, vol. 46, no. 3, pp. 983-992, 2021, https://doi.org/10.1177/0309524X211060684.

[32] P. S. Kumar, R. P. S. Chandrasena, and K. Victor Sam Moses Babu, “Design and implementation of wind turbine emulator using FPGA for stand-alone applications,” *International Journal of Ambient Energy*, vol. 43, no. 1, pp. 2397–2409, 2022, https://doi.org/10.1080/01430750.2020.1736152.

[33] S. Ashfaq *et al.*, "Comparing the Role of Long Duration Energy Storage Technologies for Zero-Carbon Electricity Systems," *IEEE Access*, vol. 12, pp. 73169-73186, 2024, https://doi.org/10.1109/ACCESS.2024.3397918.

[34] J. P. Ram, N. Rajasekar, and M. Miyatake, “Design and overview of maximum power point tracking techniques in wind and solar photovoltaic systems: A review,” *Renewable and Sustainable Energy Reviews*, vol. 73. pp. 1138–1159, 2017, https://doi.org/10.1016/j.rser.2017.02.009.

[35] N. F. Ibrahim *et al.*, “A new adaptive MPPT technique using an improved INC algorithm supported by fuzzy self-tuning controller for a grid-linked photovoltaic system,” *PLoS One*, vol. 18, no. 11, p. e0293613, 2023, https://doi.org/10.1371/journal.pone.0293613.

[36] M. M. Mahmoud, M. M. Aly, H. S. Salama, and A. M. M. Abdel-Rahim, “A combination of an OTC based MPPT and fuzzy logic current control for a wind-driven PMSG under variability of wind speed,” *Energy Systems*, vol. 13, no. 4, pp. 1075–1098, 2022, https://doi.org/10.1007/s12667-021-00468-2.

[37] B. Jing, L. Qun, L. Qiang, C. Zaiyu, H. Yuchong, and Y. Minghui, “Inertia compensation for wind turbine emulator based on anticipation deviation suppression,” *Electric Power Systems Research*, vol. 224, p. 109751, 2023, https://doi.org/10.1016/j.epsr.2023.109751.

[38] B. Yang *et al*., “Passivity-based sliding-mode control design for optimal power extraction of a PMSG based variable speed wind turbine,” *Renewable Energy*, vol. 119, pp. 577–589, 2018, https://doi.org/10.1016/j.renene.2017.12.047.

[39] M. Zerzeri, I. Moussa, and A. Khedher, “Wind turbine emulator using three-phase IM controlled through an adaptive reactive power estimator fed by soft-VSI topology,” *COMPEL - The international journal for computation and mathematics in electrical and electronic engineering*, vol. 43, no. 2, pp. 282–300, 2024, https://doi.org/10.1108/COMPEL-10-2023-0529.

[40] I. E. Maysse *et al.,* "Nonlinear Observer-Based Controller Design for VSC-Based HVDC Transmission Systems Under Uncertainties," *IEEE Access,* vol. 11, pp. 124014-124030, 2023, https://doi.org/10.1109/ACCESS.2023.3330440.

[41] M. Gannoun, J. Arbi-Ziani, and M. W. Naouar, “Modelling of a PMSG based wind turbine system with diode rectifier-based generator side converter,” *International Journal of Renewable Energy Research-IJRER*, vol. 12, no. 3, pp. 1532–1539, 2022, https://doi.org/10.20508/ijrer.v12i3.13044.g8538.

[42] Y. Cao *et al*., "A Three-Level Buck–Boost Converter With Planar Coupled Inductor and Common-Mode Noise Suppression," *IEEE Transactions on Power Electronics*, vol. 38, no. 9, pp. 10483-10500, 2023, https://doi.org/10.1109/TPEL.2023.3279987.

[43] M. M. Mahmoud, M. K. Ratib, M. M. Aly, and A. M. M. Abdel–Rahim, “Application of Whale Optimization Technique for Evaluating the Performance of Wind-Driven PMSG Under Harsh Operating Events,” *Process Integration and Optimization for Sustainability*, vol. 6, no. 2, pp. 447–470, 2022, https://doi.org/10.1007/s41660-022-00224-8.

[44] S. M. Muyeen, R. Takahashi, T. Murata and J. Tamura, "Integration of an Energy Capacitor System With a Variable-Speed Wind Generator," *IEEE Transactions on Energy Conversion*, vol. 24, no. 3, pp. 740-749, 2009, https://doi.org/10.1109/TEC.2009.2025323.

[45] S. S. Sayed and A. M. Massoud, "Review on State-of-the-Art Unidirectional Non-Isolated Power Factor Correction Converters for Short-/Long-Distance Electric Vehicles," *IEEE Access*, vol. 10, pp. 11308-11340, 2022, https://doi.org/10.1109/ACCESS.2022.3146410.

[46] M. M. Mahmoud *et al*., “Integration of Wind Systems with SVC and STATCOM during Various Events to Achieve FRT Capability and Voltage Stability: Towards the Reliability of Modern Power Systems,” *International Journal of Energy Research*, vol. 2023, no. 1, pp. 1-28, 2023, https://doi.org/10.1155/2023/8738460.

[47] G. Zhang, P. Zheng, S. Yu, H. Trinh and P. Shi, "Controllability Analysis and Verification for High-Order DC–DC Converters Using Switched Linear Systems Theory," *IEEE Transactions on Power Electronics*, vol. 36, no. 8, pp. 9678-9688, 2021, https://doi.org/10.1109/TPEL.2021.3059259.

[48] D. Zammit, C. S. Staines, A. Micallef, M. Apap, and J. Licari, “Incremental Current Based MPPT for a PMSG Micro Wind Turbine in a Grid-Connected DC Microgrid,” *Energy Procedia*, vol. 142, pp. 2284–2294, 2017, https://doi.org/10.1016/j.egypro.2017.12.631.

[49] F. Alonge, M. Pucci, R. Rabbeni, and G. Vitale, “Dynamic modelling of a quadratic DC/DC single-switch boost converter,” *Electric Power Systems Research*, vol. 152, pp. 130–139, 2017, https://doi.org/10.1016/j.epsr.2017.07.008.

[50] H. Miloudi *et al.,* "Electromagnetic Compatibility Characterization of Start-Capacitor Single-Phase Induction Motor," *IEEE Access,* vol. 12, pp. 2313-2326, 2024, https://doi.org/10.1109/ACCESS.2023.3349018.

[51] A. Fatah *et al*., “Design, and dynamic evaluation of a novel photovoltaic pumping system emulation with DS1104 hardware setup: Towards innovative in green energy systems,” *PLoS One*, vol. 19, no. 10, p. e0308212, 2024, https://doi.org/10.1371/journal.pone.0308212.